DOI: 10.17277/amt.2018.03.pp.029-036

The SHS of $Y_2Ti_2O_7$-Based Pyrochlore Ceramics

T.V. Barinova*, V.Yu. Barinov, I.D. Kovalev, N.V. Sachkova

Merzhanov Institute of Structural Macrokinetics and Materials Science, Russian Academy of Sciences, 8, Academician Osipyan St., Chernogolovka, Moscow Region, 142432, Russia;

* Corresponding author. Tel.: +7 496 52 463 04. *E-mail*: tbarinova@ism.ac.ru

Abstract

The effect of Fe and ($Al + SiO_2$) additives on the combustion mode, porosity, phase composition and structure of synthesized $Y_2Ti_2O_7$-based pyrochlore ceramic matrices. It is shown that the introduction of Fe powder does not affect the phase composition of the ceramics. The presence of aluminum in the charge led to the formation of phases of $Y_3Al_5O_{12}$ garnet and $YAlO_3$ perovskite. In the presence of the selected additives, combustion of charge billets was in a controlled stationary mode, the ceramic samples retained the shape and dimensions of the charge billet, had a cast structure, but the additives did not significantly reduce the porosity of the resulting ceramics. Ceramics with an open porosity of less than 10 % were obtained by applying an axial force of 0.1–0.3 kN per product after completing the combustion process.

Keywords

SHS ; mineral-like matrices; pyrochlore; high-level wastes.

Introduction

The research is aimed at solving the urgent problem of a closed nuclear fuel cycle – neutralization of high-level wastes (**HLWs**) containing actinides. HLWs with a high content of actinides occur during the fractionation of waste and represent the greatest nuclear threat to the environment. One of the promising approaches to the immobilization of HLWs is their isomorphic inclusion in chemically, mechanically, radiation-resistant mineral-like matrices that prevent the ingress of radionuclides into the environment [1].

This paper is a continuation of studies on the use of the SHS method for the synthesis of mineral-like matrices $Y_2Ti_2O_7$-based pyrochlore composition enriched with zirconium, and intended for immobilization of the actinide-containing fraction of HLWs [2, 3].

In the course of the study, two problems were solved: dispersion of the reaction mass in the combustion process of charge billets at atmospheric pressure and high porosity of by the SHS method ceramics produced without the use of pressing. When burning thermite compounds, the combustion temperature may exceed the melting point of the final products [4]. In this case, combustion is accompanied by a strong spread of the melt and proceeds in an explosive mode. The creation of excess gas pressure (argon, air), a decrease in the caloric content of the mixture due to dilution with oxide additives or introduction of an excess of one of the reagents into the mixture suppress the spread of the melt and transfer the combustion into a controlled stationary regime [5]. In the given combustion conditions, we failed to suppress the dispersion of the reacting mass due to the variation in the composition of the charge, the density and size of the initial billets. Earlier it was shown [3] that with increasing density of charge billets the combustion temperature T_c decreases to 1500–1470 °C. It was possible to produce ceramics that retain the shape of charge billet only with a small load of the burning sample. The combustion in this case was at the limit, as indicated by the layered structure of the product. Therefore, the dilution of the composition of the charge by the introduction of zirconium or titanium oxides to reduce the intensity of the process was not suitable, since the addition of oxides led to a further decrease in T_c. In the proposed study, attempts were made to use iron powder as additives to suppress dispersion. Iron under the investigated conditions did not form chemical compounds with the starting

compounds and combustion products and was included in the ceramic matrix in its free form due to the reduction of Fe_2O_3 iron oxide, used in the preparation of charge compositions as an oxidant. It was expected that due to the low melting point in the combustion conditions, the iron would be in the molten state, increasing the fraction of the liquid phase and contributing to a decrease in porosity. The choice of Fe_2O_3 as an oxidizer for the synthesis of ceramics was associated with the production of matrices having a lower porosity than, for example, MoO_3, under similar conditions [3]. As it is known, ceramics produced by the SHS method have a high porosity. According to the data of [6], high-porous $Y_2Ti_2O_7$-based matrices possess the necessary chemical stability, which significantly exceeds the resistance of glasses. However, it is believed that for the long-term and safe storage of HLWs, the porosity of the synthesized matrices must be reduced. To reduce the porosity, a mixture ($Al + SiO_2$) was introduced into the charge to increase the amount of the liquid phase having a reduced melting point. In addition, the presence of small amounts of aluminum in the composition of the charge should contribute to an increase in T_c due to the interaction with iron and titanium oxides proceeding with considerable heat release [7, 8].

The aim of the study was to investigate the effect of Fe and ($Al + SiO_2$) additives on the combustion regime, porosity, phase composition and structure of synthesized $Y_2Ti_2O_7$-based pyrochlore ceramic matrices enriched with zirconium. Zirconium in pyrochlore was introduced to increase its chemical and radiation resistance [9].

Experimental

Justification of the choice and procedure for calculating the charge compositions for the preparation of $Y_2Ti_{2-x}Zr_xO_7$-based ceramic matrices enriched with zirconium pyrochlore were described in [2, 3].

In the study we used: Ti of PTOM grade, TiO_2 in the form of anatase (c.p.), Y_2O_3 (c.p.), ZrO_2 (c.p.), CaO (c.p.), Fe_2O_3 III (c.p.). The indispensable components of the charge were a mechanical mixture of metal oxides, simulating the composition of real HLWs. The composition of the model mix of waste, %: CeO_2 – 25.0; La_2O_3 – 50.7; ZrO_2 – 19.6; MnO_2 – 3.8; Fe_2O_3 – 0.9. The content of model waste in the batch was 10 wt. %.

On the basis of thermodynamic calculations and experimental data, the following composition of charge (mole) was selected:

$$0.326\ Ti + 0.159Y_2O_3 + 0.102\ ZrO_2 + + 0.028\ CaO + 0.215\ Fe_2O_3 . \quad (1)$$

According to the ratio of Zr and Ti in the composition of the charge, up to 17 % of Ti atoms on Zr should be replaced in the pyrochlore structure, taking into account the introduced HLWs. The starting charge mixture was prepared by mixing in drums with steel balls. Pressing of billets was carried out on a hydraulic press. The charge compositions were pressed in the form of cylinders with a diameter of 30 and 50 mm and an average density of 2.7 g/cm^3. The pressed billets were placed in backfills of coarse-grained quartz, so as to increase the cooling time of the synthesized matrices, to reduce heat losses and to retain the shape in the event of possible melting, and to facilitate the evacuation of gases. The combustion process was initiated from the upper end of the charge billet by local heating through the ignition layer of Ti powder. Further, the combustion process spread like a pattern spontaneously in the form of a combustion wave. After passing the combustion wave, the samples were cooled under natural conditions. The SHS resulted in production of matrixes in the form of cylinders of dark gray color.

The combustion temperature T_c was determined by the thermoelectric method with the help of tungsten-rhenium thermocouples (BP-5/20) with a diameter of 200 μm. Thermocouples were installed in the center of charge billets at a distance of 5 mm from the bottom end. To measure T_c, billets with a diameter and height of 15–18 mm were used. The measurement error was 50 °C [10].

The open porosity was determined by standard methods.

The XRD was carried out on a DRON-3M ($Cu–K_\alpha$ cathode) installation. The investigation of the microstructure and local elemental analysis of the surface of ground samples were carried out using an ultra-high resolution field-emission scanning electron microscope ULTRA plus (Germany, Karl Zeiss).

Results and discussion

Ceramics sample No. 1

The charge composition No. 1 was prepared by adding 5 wt. % of Fe powder to the starting composition (1). After the SHS, no dispersion was observed, the combustion products were produced in the form of cylindrical blocks completely replicating the shape and dimensions of the initial charge billets,

while retaining the angles of the end surfaces. The samples of the products looked dense and slightly porous.

When measuring T_c of the initial charge composition (1) containing 10 % of HLWs, a value of 1500 °C was obtained, and for the composition No. 1, T_c was 1470–1480 °C. From a comparison of the obtained values of T_c, it can be seen that the addition of 5 % iron led to a decrease in T_c by 20–30 °C, which is comparable with the measurement error.

Fig. 1 shows the diffractogram of a ceramic sample No. 1. According to the XRD data (Fig. 1), the combustion product is formed by $Y_2(Ti_{0.85}Zr_{0.15})_2O_7$ pyrochlore phases, $CaTiO_3$ perovskite and metallic Fe. In the structure of pyrochlore, 15 % of Ti atoms on Zr are replaced, which is close to the ratio of the content of these elements in the charge.

The investigation of the microstructure showed that the combustion product had a cast, but porous structure. The pores were very small, and permeated the entire product, leaving practically no dense area. To illustrate Fig. 2*a–c* show photographs of the microstructure of the combustion product at various magnifications. A feature of the product obtained is the presence of two types of iron precipitates – iron, reduced from oxide in the form of fine precipitates with a size of not more than 2 μm, and iron, introduced in the form of a powder. The latter occupies rather extensive areas and is separated from the main mass of the matrix by the boundary formed by iron oxide. Obviously, initially the particles of the powder of the iron used were covered with an oxide film that was not recovered during the synthesis. In Fig. 2*b* in the upper part of the photo a particle of iron separated from the bulk of the ceramic by a dark strip of oxide film is

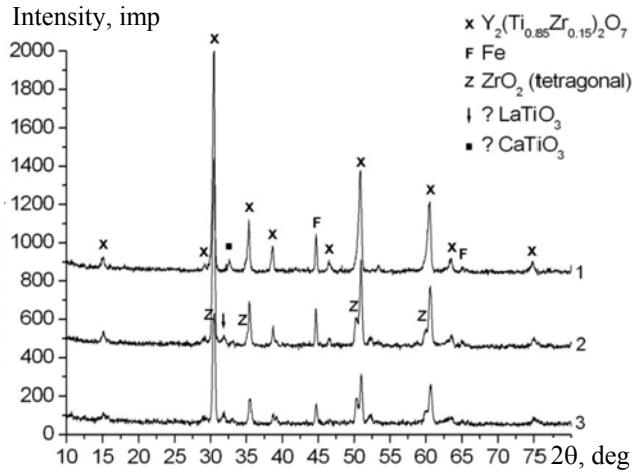

Fig. 1. Diffractograms of ceramics produced by combustion of compositions No. 1, 2, 3

shown. Fig. 2*c* clearly shows three phase components of the oxide phase, which are in close contact. According to the analysis, the oxide phase is based on rounded pyrochlore grains, which form microcrystalline aggregates of gray color (Fig. 2*c*). A feature of the obtained structure is also the absence of pyrochlore grains with a ring structure, which was observed in all our previous studies, regardless of which oxide was chosen as the oxidizer – Fe_2O_3 or MoO_3. There are no interlayers of other phases between the pyrochlore grains in microcrystalline aggregates. It can be seen that the pyrochlore grains, as well as the perovskite grains, differ in color, indicating variations in their composition. Thus, the composition of pyrochlore at point *5* is more enriched in zirconium than at point *6*. Perovskite grains located in close intergrowth with pyrochlore have a light gray color.

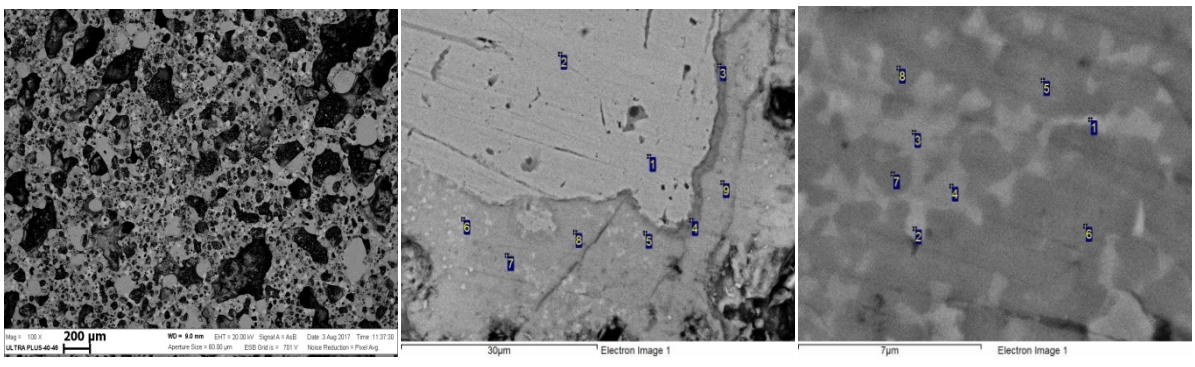

a) *b*) *c*)

Fig. 2. Microstructure of the product of composition No. 1 at different magnifications:
a – × 100; *b* – × 5000; *c* – × 20 000;
b: *1*, *2* – Fe; *3*, *4* – Fe oxide, $CaTiO_3$ perovskite; *5*, *6* – $CaTiO_3$ perovskite; *7 – 9* –$Y_2Ti_2O_7$ pyroclore;
c: *1* – Fe; *2* – $LaTiO_3$ perovskite; *3*, *4* –$CaTiO_3$ perovskite; *5 – 8* – pyroclore

Distribution of elements (at. %) in Fig. 2*b*

Spectrum	O	Al	Si	Ca	Ti	Mn	Fe	Y	Zr	La	Ce
1	3.4	1.8	0.1	0.0	0.5	0.0	93.8	0.0	0.1	0.1	0.1
2	2.8	2.2	0.4	0.1	0.0	0.0	93.5	0.2	0.3	0.2	0.2
3	62.2	0.7	0.1	0.1	1.8	0.2	32.5	1.7	0.4	0.1	0.1
4	60.7	1.0	0.0	0.1	0.6	0.0	36.9	0.4	0.0	0.0	0.1
5	67.1	0.9	0.5	1.8	11.5	0.2	4.1	9.1	0.8	2.8	1.1
6	41.3	1.6	0.7	0.9	5.7	0.0	40.8	5.7	1.3	1.4	0.6
7	66.9	0.6	0.9	0.8	11.8	0.2	2.3	13.5	1.8	0.6	0.5
8	65.1	0.6	0.6	0.8	13.5	0.1	1.6	14.8	1.4	0.8	0.5
9	66.0	0.7	0.8	0.6	13.5	0.0	0.9	14.6	1.7	0.6	0.5

Distribution of elements (at. %) in Fig. 2*c*

Spectrum	O	Ca	Ti	Mn	Fe	Y	Zr	La	Ce
1	36.7	0.3	6.3	0.0	46.0	8.8	1.1	0.5	0.2
2	69.6	1.0	9.2	0.4	5.0	11.4	0.6	1.8	1.1
3	65.2	3.1	11.3	0.2	5.9	9.8	0.5	2.7	1.4
4	66.9	2.2	11.3	0.4	4.4	10.8	0.7	2.1	1.2
5	67.6	0.5	13.1	0.1	1.5	14.3	1.3	1.0	0.8
6	69.2	0.5	12.7	0.0	1.1	14.4	1.0	0.6	0.5
7	66.8	0.9	13.1	0.1	3.5	13.1	0.9	1.0	0.7
8	69.4	0.6	12.8	0.0	1.5	13.6	0.7	1.0	0.6

Both phases are chemically solid solutions of several components, including rare-earth elements (**REEs**) from the model mixture of HLWs. The content of REEs in perovskite phases was much higher than in pyrochlore.

The fine grain size of the phase constituents of ceramics No. 1 and the ceramics studied below does not allow us to establish their exact composition due to the capture of neighboring regions of the matrix by the electronic probe, which makes it difficult to calculate the real formulas of the phases formed.

Ceramics sample No. 2

The structure of titanate pyrochlore is stable with a content of up to 30 % zirconium in its lattice [11], and according to XRD data, 15 % of Ti atoms on Zr are replaced in the structure of pyrochlore as a result of synthesis. To increase the share of substitution, addition of 5 mass.% of ZrO_2 was introduced into the composition of charge No. 1, which should lead to an increase in the chemical and radiation resistance of pyrochlore. Also, 4 % of the mixture ($Al + SiO_2$) was introduced into the charge mix, while the Fe fraction decreased to 2.5 % by weight. The selection of the composition was carried out experimentally.

Fig. 1 shows the diffraction pattern of product No. 2. Five phases can be distinguished in the product: $Y_2(Ti_{0.85}Zr_{0.15})_2O_7$ pyrochlore, $CaTiO_3$ perovskites and $LaTiO_3$, ZrO_2 and Fe. According to the XRD data, the amount of zirconium in the pyrochlore structure due to the additional addition of ZrO_2 did not increase, while ZrO_2 remained in the combustion product as an independent phase.

A study of the structure showed that the product was porous; the pores were larger than in sample No. 1. Iron was represented by two types of excreta: large secretions surrounded by a dark border of iron oxide belonging to the introduced gland and small, not exceeding 2 μm round precipitates belonging to the reduced iron. There were also large iron deposits of regular round shape, around which pores were formed.

The pyrochlore grains had a rounded shape and a weakly expressed annular structure – a dark center and a lighter border region, and separated from each other by phase interlayers of a darker color. The dark-colored phase can belong to the perovskite $YAlO_3$. Perovskite grains contained a higher percentage of rare earth elements than pyrochlore.

Fig. 3*c* shows a section of the ceramic where the region with unreacted Y_2O_3 is visible (point *1*). A dense ring of the gray phase is formed around Y_2O_3. It is possible that the gray ring belongs to the $YAlO_3$ alumium yttrium perovskite, in which a high percentage of rare-earth elements and Si was noted.

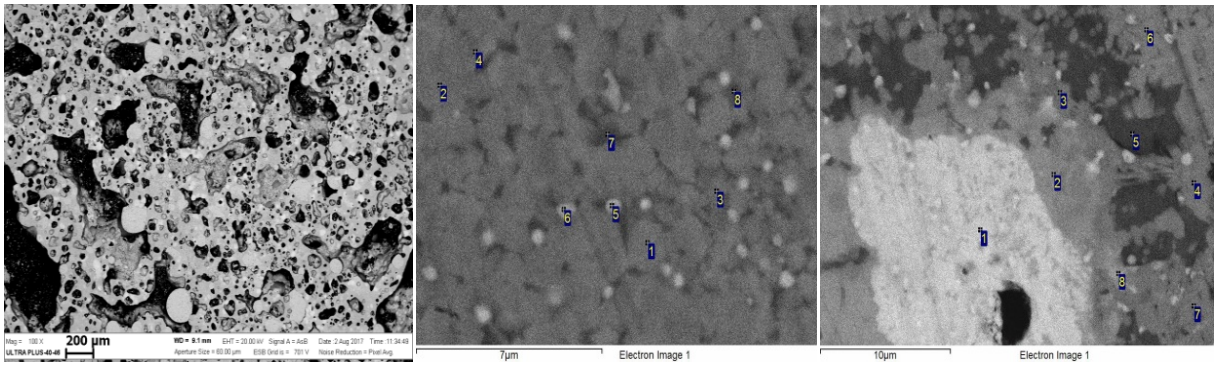

a) *b*) *c*)

Fig. 3. Microstructure of the product of composition No. 2 at different magnifications:
a – × 100; *b* – × 5000; *c* – × 20 000;
b: *1 – 4* –Y_2Ti_2O7 pyrochlore; *5*, *6* – Fe; *7*, *8* –$YAlO_3$ perovskite;
c: *1* – Y_2O_3; *2*, *8* – $YAlO_3$ perovskite; *3*, *4*, *6*, *7* – YAlO3 pyrochlore; *5* – гранат$Y_3Al_5O_{12}$ garnet

Distribution of elements (at. %) in Fig. 3*b*

Spectrum	O	Al	Si	Ca	Ti	Mn	Fe	Y	Zr	La	Ce
1	67.4	2.2	1.1	0.5	9.9	0.0	0.5	13.1	3.9	0.6	0.7
2	66.4	2.2	1.2	0.4	10.7	0.1	0.3	14.1	3.4	0.7	0.5
3	70.0	3.5	1.2	0.5	8.9	0.0	0.7	9.9	4.4	0.3	0.5
4	63.1	2.9	1.4	0.4	11.5	0.1	0.8	14.5	3.3	1.0	0.8
5	53.6	3.7	1.7	0.4	7.1	0.4	18.8	10.1	2.6	0.9	0.6
6	49.0	3.2	1.5	0.4	8.3	0.1	20.6	12.0	2.9	0.9	0.8
7	66.9	6.5	3.6	1.2	6.1	0.2	1.3	8.8	2.2	1.9	1.2
8	65.4	5.5	2.9	1.1	7.0	0.3	2.4	9.4	3.1	1.6	1.1

Distribution of elements (at. %) in Fig. 3*c*

Spectrum	O	Al	Si	Ca	Ti	Mn	Fe	Y	Zr	La	Ce
1	62.7	0.8	1.5	0.3	0.3	0.0	0.8	32.9	0.1	0.3	0.0
2	65.2	2.0	8.7	1.1	2.3	0.2	0.2	16.6	0.8	1.7	1.0
3	64.4	3.1	1.4	0.5	11.4	0.1	1.5	13.9	1.9	0.7	0.7
4	68.2	1.5	1.4	0.3	10.9	0.0	0.1	14.3	2.2	0.6	0.5
5	66.0	16.7	1.2	0.6	1.8	0.2	0.4	12.6	0.5	0.0	0.0
6	66.0	1.8	1.6	0.5	11.2	0.3	0.4	13.2	2.9	1.0	0.9
7	65.6	2.5	2.4	0.4	11.6	0.0	0.6	12.8	1.5	1.5	1.0
8	66.7	2.5	7.5	2.1	3.5	0.3	1.2	10.9	0.9	2.5	1.7

Then comes the ring, consisting of a dark color phase (point *5*), it can belong to the $Y_3Al_5O_{12}$ alumina garnet. The formation of the garnet phase under synthesis conditions is possible at a temperature of 1250–1400 °C according to the following reaction [12]:

$$3YAlO_3 + Al_2O_3 \rightarrow Y_3Al_5O_{12}.$$

Judging from the analysis, the $Y_3Al_5O_{12}$ phase contained the minimum amount of lanthanum and cerium, compared with the phases of perovskites (points *2*, *8*) and pyrochlore (points *3*, *4*, *6*, *7*).

The investigation of the structure showed that the phase of the garnet was distributed in the sample of the ceramic not uniformly, but forms microcrystalline aggregates consisting of intergrown grains without interlayers of other phases between them.

To prove the formation of $Y_3Al_5O_{12}$, the amount of Al in the charge was increased to 4 %. The interpretation of the diffractogram of the synthesized ceramics in this case in Fig. 4 confirmed the formation of the $Y_3Al_5O_{12}$ phase.

Ceramics sample No. 3

This composition of charge differs from the previous one by the absence of Fe powder in the charge. The measurement of T_c for a given composition showed values of 1550–1580 °C.

According to the XRD data (Fig. 1), the phase composition of the obtained product was the same as for composition No. 2. The structure of this product differed from the others in the presence of rare but large pores. Reduced iron in some areas formed large discharge with a size of more than 200 microns,

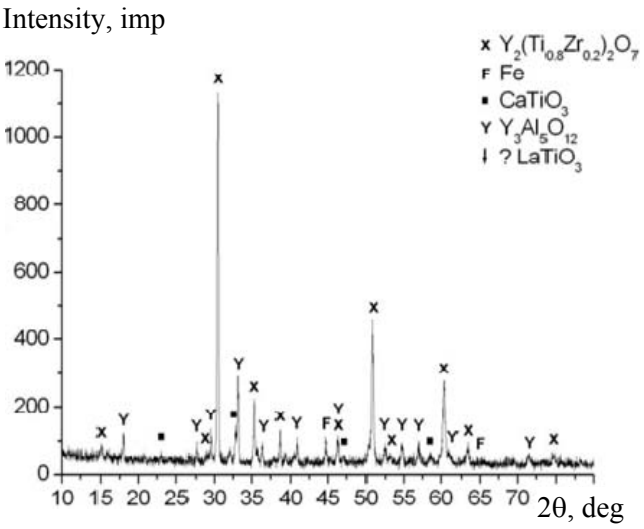

Fig. 4. Diffractogram of the ceramics sample No. 4

indicating a higher T_c in this composition compared with the previous ones (Fig. 5*b*). In Fig. 5*b* the microstructure of the region of the matrix consisting of the following phases is represented: pyrochlore, $LaTiO_3$ perovskite, ZrO_2 and Fe. Probably points *7* and *8* belong to the phase of the grenade. The section of the matrix with a larger magnification is shown in Fig. 5*c*. The maximum amount of lanthanum and cerium is contained in the perovskite phase (points *3* and *4*), the minimum amount in the pyrochlore phase.

In all three compositions, the additives were added in excess of the stoichiometry of the original composition according to equation (1). With an increase in the content of iron oxide composition No. 3 in the charge in the amount necessary for the reaction with aluminum, the $Fe_2Al_2O_4$ phase was formed in the combustion products.

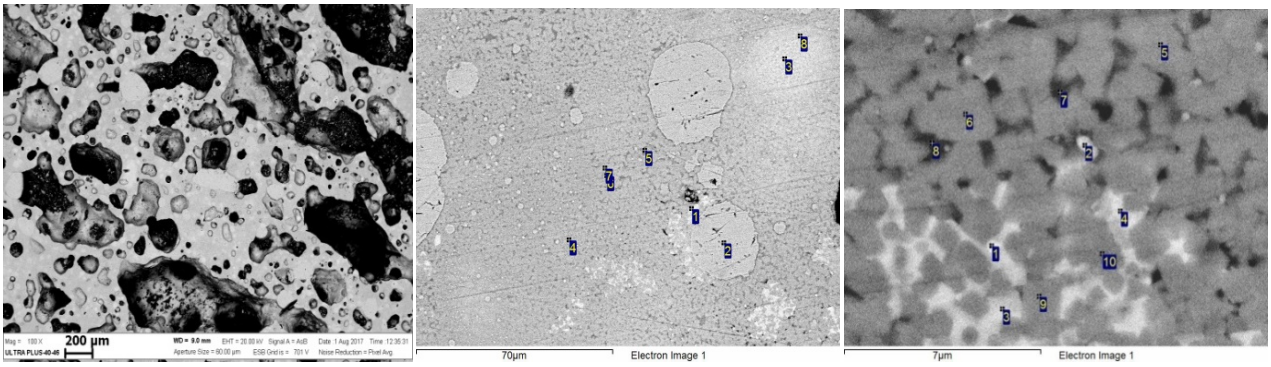

a) *b*) *c*)

Fig. 5. Microstructure of the product of composition No. 3 at different magnifications:
a – × 100; *b* – × 5000; *c* – × 20 000;
b: *1*, *5* – $LaTiO_3$ perovskite; *2* – Fe; *3*, *8* – ZrO_2 region; *4*, *7* – $Y_2Ti_2O_7$ pyrochlore
(point *6* is not identified because it coincides with point *7*);
c: *1*, *2* – Fe; *3*, *4* – $LaTiO_3$ perovskite; *5*, *6*, *9*, *10* – $Y_2Ti_2O_7$ pyrochlore; *7*, *8* – $Y_3Al_5O_{12}$ garnet

Distribution of elements (at. %) in Fig. 5*c*

Spectrum	O	Al	Si	Ca	Ti	Mn	Fe	Y	Zr	La	Ce
1	42.2	2.6	0.8	0.8	9.7		30.3	8.2	1.3	1.9	2.0
2	46.8	3.8	1.9	0.4	9.2		23.2	10.8	2.1	0.8	0.9
3	65.0	2.6	0.5	1.3	13.4	–	0.5	9.2	1.6	3.2	2.6
4	66.2	3.7	0.5	1.4	12.0		1.0	7.2	1.3	3.5	3.1
5	65.2	1.9	1.4	0.5	12.3		0.5	13.4	3.0	0.7	1.1
6	66.5	1.6	1.2	0.4	12.0		0.7	13.4	2.6	0.5	0.8
7	68.8	5.0	3.0	0.6	8.0	0.1	1.2	8.8	1.7	1.5	1.2
8	67.0	6.8	3.7	1.0	7.1	0.1	2.0	7.4	1.6	1.8	1.5
9	64.8	1.2	0.8	0.4	13.5	–	1.0	13.3	2.7	0.9	1.3
10	65.3	1.6	0.7	0.6	13.7		0.4	12.9	2.4	0.9	1.4

It is shown that the open porosity of the first two ceramics was 40 %. Below are the values for the last composition – 30 %. To produce ceramics with low porosity, after complete passage of the synthesis, the hot combustion products were manually sealed. When a single axial force of 0.1–0.3 kN was applied with the help of a piston made of BN, they were significantly compacted. The values of open porosity were less than 10 %. Fig. 6 shows the structure of the ceramic after sealing in a hot state. For comparison: using the SHS compaction method (pressure pressing on the non-heated combustion product was 100 MPa), the open porosities of synthesized pyrochlore-based ceramics were 2.4–4.0 % [13].

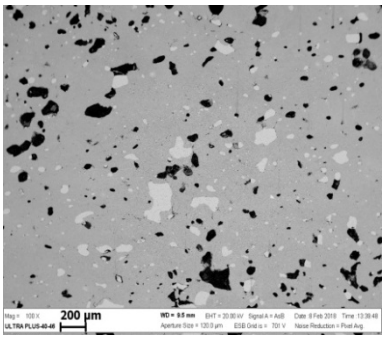

Fig. 6. Microstructure of the ceramic sample after compaction (open porosity 8 %)

Fig. 7. Photo of a typical sample of ceramics

Fig. 7 shows a photo of a typical sample of ceramics produced by SHS without applying pressure.

Conclusion

The effect of Fe additives and mixtures ($Al+SiO_2$) on combustion in the SHS regime in the air of pressed batch blanks on the basis of the composition $CaO + Y_2O_3 + ZrO_2 + Ti + Fe_2O_3$ was studied. It is shown that additives added to the charge contribute to the conversion of the combustion reaction to a controlled stationary regime. The produced samples of ceramics completely retain the shape and dimensions of the initial charge billets. However, the resulting ceramic had a high porosity. It was possible to obtain ceramics with open porosity values of less than 10% only when the load applied to combustion products in the hot state.

Acknowledgments

The research was financially supported by the Russian Foundation for Basic Research (*project no. 16-53-00084*). *The work was performed using a set of modern scientific instruments available for multiple accesses at the ISMAN Center of Shared Services.*

References

1. Stefanovsky S.V., Yudintsev S.V. Titanates, zirconates, aluminates and ferrites as waste forms for actinide immobilization. *Russian Chemical Reviews,* 2016, vol. 85(9), p. 962. doi: org/10.1070/RCR4606

2. Barinova T.V., Podbolotov K.B., Borovinskaya I.P., Shchukin A.S. Self-propagating high-temperature synthesis

of ceramic matrices for immobilization of actinide-containing wastes. *Radiochemistry*, 2014, vol. 56, issue 5, pp. 554-559. doi: 10.1134/S1066362214050178.

3. Barinova T.V., Borovinskaya I.P., Barinov V.Yu., Kovalev I.D., and Podbolotov K.B. SHS of $Y_2Ti_2O_7$-Based Mineral-Like Ceramics: Influence of Green Density, *Int. J. Self-Prop. High-Temp. Synth.*, 2017, vol. 26, issue 2, pp.119-123. doi: 10.3103/S1061386217020030.

4. Tarakanov A. Yu., Shiryaev A. A., Yukhvid V.I. Fazovye prevrashheniya v vysokokalorijnykh geterogennykh sistemakh okisel – vosstanovitel' – nemetall [Phase transformations in high-caloric heterogeneous oxide-reduction-non-metal systems]. *FGV*, 1991, vol. 27, issue 3, pp. 68-74. (Rus)

5. Gorshkov V.A., Sanin V.N., Yukhvid V.I., Modelirovanie kriticheskikh uslovij v rabochej yachejke atomnogo reaktora s pomoshh'yu goreniya vysokoehnergeticheskikh SVS-sistem [Modeling of Critical Conditions in a Fuel Cell of a Nuclear Reactor Based on Combustion of Energetic SHS Systems]. *FGV*, 2014, vol. 50, issue 4, pp.42-4. (Rus)

6. Vinokurov, S.E., Kulyako, Yu.M., Perevalov, S.A., Myasoedov, B.E., Immobilisation of actinides in pyrochlore-type matrices produced by self-propagating high-temperature synthesis, *C. R. Acad. Sci., Ser. Chimie*, 2007, issue. 10, pp.1128-1130. doi: 10.1016/j.crci.2007.04.011

7. Kobyakov V.P., Barinova T.V., Mashkinov L.B., and Sichinava M.A. Heat Release in the Preparation of TiC–Al2O3 Ceramics. *Inorganic Materials*, vol. 48, issue 5, pp. 549-551. doi: 10.1134/S0020168512040061.

8. Chernenko E.V, Afanas'eva L.F., Lebedeva V.A., Rozenband V.I., Vosplamenyaemost' smesej okislov metallov s alyuminiem [The flammability of mixtures of metal oxides with aluminum]. *FGV*, 1988, vol. 24, issue 6, pp.1-3. (Rus)

9. Wang S.X., Begg B.D., Wang L.M., Ewing, R.C., Weber W.J., and Govidan Kutty K.V. Radiation stability of gadolinium zirconate: A waste form for plutonium disposition, *J. Mater. Res*., 1999, vol. 14, no. 12, pp. 4470-4473.

10. Maslov V.M., Borovinskaya I.P., Merzhanov A.G. Ehksperimental'noe opredelenie maksimal'nykh temperatur protsessov samorasprostranyayushhegosya vysokotempera-turnogo sinteza [Experimental determination of the maximum temperatures of processes of self-propagating high-temperature synthesis]. *FGV*, 1978, issue 5, pp. 79-85. (Rus)

11. Yudintsev S.V., Stefanovskii S.V., and Chou S., Phase formations in Ca–Ce–Ti–Zr–(Hf)–O systems and optimization of synthesis conditions for pyrochlore based actinide matrices, *Fiz. Khim. Obrab. Mater.*, 2008, no. 3, pp. 70-80.

12. Nejman A.YA., Tkachenko E.V., Kvichko L.A., Kotok L.A. Usloviya i makromekhanizm tvyordofaznogo sinteza alyuminatov ittriya [Conditions and macromechanism of solid-phase synthesis of yttrium aluminates]. *Zhurnal neorganicheskoj khimii*, 1980, vol.25, issue 9, pp. 2340-2345. (Rus)

13. Barinova T.V., Borovinskaya I.P., Ratnikov V.I., Ignat'eva T.I., Belikova A.F. Samorasprostranyayushhijsya vysokotemperaturnyj sintez (SVS) keramiki na osnove pirokhlora dlya immobilizatsii dolgozhivushhikh vysokoaktivnykh otkhodov [Self-propagating high-temperature synthesis (SHS) of pyrochlore-based ceramics for the immobilization of long-lived high-level waste]. *Radiokhimiya*, 2013, vol. 55, issue 6, pp. 539-543. (Rus)